Biomedical Physics & Engineering Express

PAPER

Optimal pulse configuration for peripheral inductive nerve stimulation

J Rapp[1,3], P Braun[1,3], W Hemmert[1,2] and B Gleich[1]

[1] Munich Institute of Biomedical Engineering (MIBE), Technische Universität München, Garching 85748, Germany
[2] Bio-inspired Information Processing (BAI), Technische Universität München, Garching 85748, Germany
[3] These authors contributed equally to this work.

E-mail: jonathan.rapp@tum.de

Keywords: peripheral stimulation, magnetic stimulation, pulse duration, pulse shape, neuronal simulation

OPEN ACCESS

RECEIVED
14 December 2021

REVISED
3 January 2022

ACCEPTED FOR PUBLICATION
8 February 2022

PUBLISHED
18 February 2022

Abstract

Peripheral magnetic stimulation is a promising technique for several applications like rehabilitation or diagnose of neuronal pathways. However, most available magnetic stimulation devices are designed for transcranial stimulation and require high-power, expensive hardware. Modern technology such as rectangular pulses allows to adapt parameters like pulse shape and duration in order to reduce the required energy. Nevertheless, the effect of different temporal electromagnetic field shapes on neuronal structures is not yet fully understood. We created a simulation environment to find out how peripheral nerves are affected by induced magnetic fields and what pulse shapes have the lowest energy requirements. Using the electric field distribution of a *figure-of-8* coil together with an axon model in saline solution, we calculated the potential along the axon and determined the required threshold current to elicit an action potential. Further, for the purpose of selective stimulation, we investigated different axon diameters. Our results show that rectangular pulses have the lowest thresholds at a pulse duration of 20 μs. For sinusoidal coil currents, the optimal pulse duration was found to be 40 μs. Most importantly, with an asymmetric rectangular pulse, the coil current could be reduced from 2.3 kA (cosine shaped pulse) to 600 A. In summary, our results indicate that for magnetic nerve stimulation the use of rectangular pulse shapes holds the potential to reduce the required coil current by a factor of 4, which would be a massive improvement.

1. Introduction

Magnetic stimulation has a wide field of applications, including the treatment of mental illness [1, 2] as well as the examination of conduction between motor cortex and muscles [3]. The most prominent application of magnetic stimulation is transcranial magnetic stimulation (TMS), which is already deployed in numerous therapies [4–7].

Magnetic stimulation of peripheral nerves has been examined in several studies. Promising applications are for example rehabilitation therapy [8–10] or stimulation of the phrenic nerve [11, 12]. In peripheral stimulation, the use of magnetic fields is often compared to the use of electric fields generated by electrodes. Extensive advantages are non-invasive application and less pain [11–14]. However, considerably more energy is required to evoke a comparable electric field. Despite the considerable advantage of peripheral magnetic stimulation, it is not yet commonly used in clinical settings.

Reasons for that might be insufficient adaption to specific applications or too expensive and complex stimulation devices. Most stimulation devices available on the market are operated with high currents of up to 10 kA [15] with the consequence of being large and costly. Such complexity might be unnecessary for the excitation of muscular groups, by stimulating the corresponding motor neurons in the peripheral nervous system. Motor neurons are large and hence easier to stimulate, compared to thinner axons [16–23]. Motor neurons innervate muscles and can be represented in the Erlanger-Gasser Classification as $A\alpha$ and $A\gamma$ fibres [23]. Typical diameters of these types are 5μm to 20 μm. Nociceptors and thermoreceptors, sensory fibres responsible for pain and temperature, respectively, have smaller diameters in the range of 1 μm to 5 μm and are classified as $A\delta$ or C fibres. By

adapting the stimulation pulse intensity and duration, it is possible to selectively stimulate functional groups within a nerve and avoid potential side effects resulting from the activation of neighboring nerve fibers. Approaches to address those requirements have been conducted by [13, 16, 20].

When it comes to stimulation energy and selective stimulation, the temporal electric field pulse is a crucial parameter. It is directly related to the temporal derivative of the coil current. Hence, it is limited by the device circuitry, where coil and capacitors are the most important elements. However, the introduction of more recent devices like flexTMS or cTMS allows for a more flexible adaptation of the current pulse [24, 25]. The question arises whether sinusoidal or triangular current pulses are favourable and which pulse duration is ideal. Rectangular electric field shapes have been reported to be beneficial in stimulating neuronal structures [26–28]. Yet, comparing sinusoidal and rectangular pulses is challenging, as the former consist of equal hyper- and depolarizing phases, while the phases of the latter can be adjusted individually by varying the strength and duration of the pulse intensity. Further, a rectangular pulse carries more energy than a cosine wave of the same duration.

Concerning pulse duration, chronaxie is an established measure for temporal properties of neurons [29]. It can be determined based on the required field strength for varying pulse duration (strength-duration curves). For pulses longer than chronaxie times the resistive part of the neuron membrane becomes dominant and pulse energy will be lost. Therefore, short pulses are preferable, which can be more easily achieved by using cTMS devices [26, 30, 31].

Experimental investigations have been conducted on strength-duration relations [22, 32, 33] and different pulse shapes [31, 34–36]. However, an overall comparison is hardly possible due to the use of various stimulation devices and target sites. Another suitable approach to acquire a deeper understanding of the field distribution and its effect on nerves are neuronal simulations. Approaches using these simulations to provide a more extended insight into the impact of pulse durations and different axon diameters have been conducted [16, 19, 33]. Further simulation work has been done on the impact of spatial field distribution on peripheral nerves [13, 37, 38]. Nonetheless, a comparison including all relevant pulse shapes and the corresponding strength-duration curves has not been published so far. Our goal is to get a deeper understanding of the impact of different pulse shapes on peripheral stimulation with magnetic fields. Moreover, we want to discuss how the use of various temporal field shapes can potentially reduce energy requirements for the stimulation. The goal is to find optimized parameters for the efficient stimulation of peripheral nerves. The spatial field distribution of a *figure-of-8* coil is coupled to a model representing the target neuron. By combining the field distribution with a temporal vector, the potential along the axon was calculated. To account for the impact on different axon types we employed various axonal models each for different axon diameters. Finally, using the NEURON environment, we evaluated current thresholds for all pulse shapes and calculated the required coil current.

2. Methods

2.1. Electrical field

Coil geometry and current determine the strength, temporal and spatial shape of the electric field. Among other important parameters such as axon geometry and the positioning in relation to the coil, these are the governing parameters responsible for the energy required to excite a neuron. The electric field data is generated in the low frequency magnetostatic Solver of CST (Dassault Systèmes Simulia). It uses the finite-elements-method, the finite integration technique and the transmission-line matrix method (TLM) to provide efficient and effective solvers for the Maxwell equations. In this work the relative spatial distribution of the electric field is mostly independent of the used current shape, since the influence of higher frequencies is negligible. Hence, it is possible to decouple the spatial distribution and the temporal component of the electric field. The field was calculated using a sinusoidal current with a specific coil current frequency of 10 kHz to get the relative spatial distribution of the electric field. The resulting electric field data can then be adjusted using Faraday's law of induction

$$\mathcal{E} = -\frac{\mathrm{d}\Phi_B}{\mathrm{d}t} = -\frac{\mathrm{d}}{\mathrm{d}t}(LI) = -L\frac{\mathrm{d}I}{\mathrm{d}t}, \tag{1}$$

where $\mathcal{E}$ is the electromotive force related to the conservative electrostatic field by $\mathcal{E} = -\int_A^B E_{cs} \cdot \mathrm{d}l$, Φ_B is the magnetic flux, I represents the coil current and L the coil inductance.

The pulse duration depends on the coil current frequency. For example, a biphasic current pulse of 10 kHz results in an overall pulse duration of 100 μs. Hence, for pulse durations other than 100 μs the field strength must be scaled according to equation (1). The thresholds in the strength-duration curves are scaled as:

$$I_{\mathrm{coil}} = I_{\mathrm{sim}} \cdot \frac{T_{\mathrm{D}}}{T_{\mathrm{ref}}} \cdot N, \tag{2}$$

where I_{sim} is the threshold current based on the field strength of a 10 kHz coil current, T_{D} is the duration of the depolarizing phase of the pulse, T_{ref} is 100 μs, corresponding to a coil current frequency of 10 kHz and N is the number of cycles within the pulse. For example, N equals 1 for a *Cosine* or 0.5 for a $\frac{1}{2}$ *Cosine* pulse (see figure 2). Discussing magnetic stimulation, the term pulse shape often refers to the coil current. However, in this paper we are rather interested in the temporal electric field shape. Hence, when talking

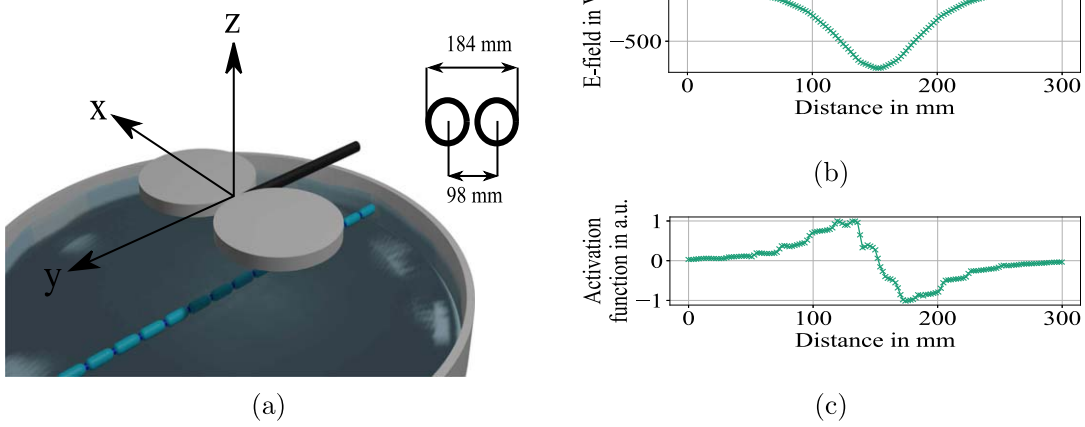

Figure 1. (a) Position of a *figure-of-8* coil in relation to a long, myelinated axon in saline solution with coordinate system; the coil dimensions are shown on the right side, the diameter of a single coil segment is 43 mm; the distance between coil and axon is 27 mm; (b) Electric field E_y at the nodes along the axon; (c) Activation function at the nodes.

about pulse shapes, we refer to the electric field. Figure 2 shows a list of pulse shapes which can be produced with common stimulation devices. For example, a cosine-shaped pulse corresponds to a sinusoidal coil current. Further, we compared rectangular pulses, which are generated by triangular current shapes. In order to get a better insight into the effect of electromagnetic fields on neuronal structures, we also investigated idealized pulse shapes which do not correspond to any available stimulation device.

We used the electric field induced by a *figure-of-8* coil in saline solution. The diameter of each coil segment is 86 mm and the spacing between the two coil segments is 12 mm (figure 1). Those dimensions are similar to commercially available coils (magstim D70, 90 mm coil diameter; MagVenture C-B70, 97 mm; MagVenture C-B60, 75 mm). The coil is positioned at a distance of 27 mm to the axon. The electric field along the axon is shown in figure 1. The likeliest position of the axon to be activated depends on the spatial gradient of the electric field distribution, which is described by the activation function [39]. Due to symmetry features of the applied coil, the field is symmetric along the fibre. As demonstrated in figure 1, the activation function is symmetric as well, with different polarities. Hence, threshold calculations are independent of polarity because both polarities are present.

2.2. Neuronal model

The description of axonal dynamics using electrical models is based on the research of Hodgkin and Huxley [40]. Unmyelinated axons are simulated using the Hodgkin-Huxley model for giant squid axons, whereas myelinated axons require some modifications. For mammalian peripheral nerves, the Richardson-McIntyre-Grill (RMG) model is well established [41]. Both models consist of capacitors and voltage controlled resistors representing the ion channels. In order to simulate myelinated fibres we used a modified Hodgkin-Huxley model (MHH), which takes myelin sheaths into account, and the RMG double cable model, since it better reflects mammalian myelinated fibres [41]. In particular, non-linearities occurring at brief pulses are modelled more precisely. Disadvantages of this approach are higher complexity and time consuming computing. All models were created using NEURON [42] and have a compartment structure where each section has individual properties, depending on its membrane characteristics. The MHH model consists of two different sections, Nodes of Ranvier and myelin sheaths, where the latter ones have near insulating membranes. The RMG model contains the same Nodes of Ranvier. However, the myelinated sections are split up to six different sections to account for the distinct segments of a myelin sheath.

2.3. Coupling field to axon model

The axon is positioned in y-direction, as shown in figure 1. For straight peripheral nerves, only the parallel component of the electric field is relevant to trigger an action potential [37]. Using the electric field distribution (E_y) calculated for saline solution the potential along the axon is determined, shown in figure 1.

Hence, the potential at each axon segment is calculated by integrating the electric field along the nerve [37, 43, 44]. With respect to the compartmental structure, the potential is calculated for each section in dependence of the previous section:

$$\phi_{\mathrm{i}} = \phi_{\mathrm{i}-1} - \frac{\vec{E}_{\mathrm{i}} + \vec{E}_{\mathrm{i}-1}}{2} \cdot \vec{s}, \tag{3}$$

where ϕ is the electric potential, $\vec{E}$ is the electric field in direction of the axon and $\vec{s}$ is the displacement vector between two segments. The indices i and $i-1$ describe the current and previous segment, respectively [37].

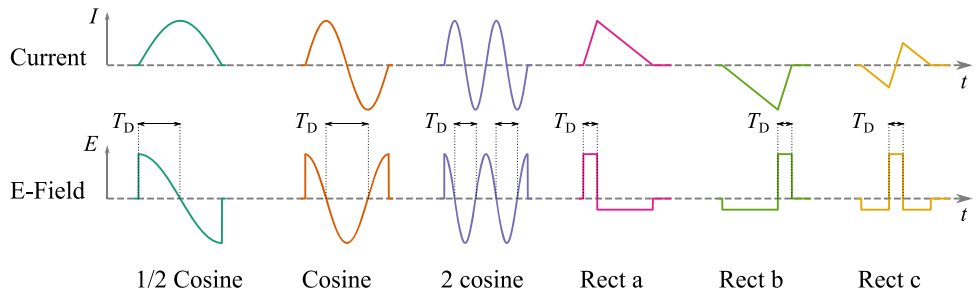

Figure 2. Overview of temporal electric field shapes which correspond to the derivative of the coil current. Cosine-shaped pulses arise from sinusoidal coil currents while rectangular field pulse configurations are induced by triangular coil currents. T_D describes the depolarizing phase of the pulse.

To take the temporal change of the electric field into account, the acquired potential is scaled with the waveform of the desired pulse shape, demonstrated in figure 2. To describe the membrane potential V_m along the cell, the cable equation for external electric fields must be solved [37, 45]. Thus, the potential over time acquired from equation (3) and the stimulus vector is applied to NEURON's extracellular mechanism to solve the cable equations.

2.4. Experiments

In our experiments we determined the threshold coil current for different pulse shapes and durations as well as various axon diameters. In order to find stimulation thresholds, the initial electric field distribution is multiplied stepwise by a factor until an action potential propagates in both directions of the axon. This criterion is fulfilled as soon as the membrane potential of the first and last axon section is depolarized to 15 mV. Subsequently, the coil current is calculated from the required field strength using equation (1).

In the first experiments, we investigated strength-duration relations for several pulse shapes (see figure 2). The pulse duration T_D was varied between 10 μs and 500 μs. We employed RMG and MHH axons of 12.8 μm diameter and 300 mm length. The axon was placed at the coil centre in y-direction (figure 1) with a distance of 27 mm, which is a realistic distance between coil and fibre.

Common parameters to assess pulse durations of rectangular pulses are chronaxie time and rheobase. The latter one is the lowest achievable threshold field strength at long pulse durations. Chronaxie is the pulse duration where twice the rheobase current is required. Analogously, we used the strength-duration curves of the required electric field intensity (see supplementary) to determine the lowest possible field strength, as well as the pulse duration which requires twice as much field strength for each stimulus. Chronaxie times for axons can be calculated based on the axon time constant τ [29], using the quantity:

$$t_{\text{Chronaxie}} = -\tau \ln(0.5). \quad (4)$$

τcan be calculated using the nodal leakage conductance and the membrane capacitance, which results in 285.7 μs for a 12.8 μm axon.

In further experiments, we analysed different configurations for the positive and negative part of rectangular pulse shapes (figure 4). *Rect a* and *Rect c* pulses were compared at pulse durations of 10 μs, 30 μs and 150 μs. Thresholds are given in relation to an ideal rectangular pulse of the corresponding duration.

Moreover, we conducted experiments comparing pulse duration and stimulus shapes on several axon diameters. We varied the pulse duration from 40 μs to 400 μs for RMG axons of 16 μm, 12.8 μm, 8.7 μm and 5.7 μm. The axon length was set to 200 mm. Again, the axon was placed in y-direction at the centre of the coil with a distance of 27 mm. The thresholds for different stimuli are given in relation to the threshold required for an ideal rectangular pulse, and the thresholds for pulse duration variations are given relative to the threshold required for a diameter of 16 μm.

3. Results

3.1. Cosine pulses

We compared three cosine-shaped pulses: $\frac{1}{2}$ *Cosine*, *Cosine* and *2 Cosine*, demonstrated in figure 2. The corresponding strength duration curves are shown in figure 3. The curves are scaled depending on pulse duration according to equation (2).

As shown in figure 3, the required coil current is higher for long pulse durations as well as for pulses shorter than 75 μs. The minimum achievable currents and the corresponding pulse widths are given in table 1 for each pulse shape. Using the RMG model, the lowest threshold was 5.7 kA and was achieved with a *2 Cosine* pulse while the MHH model predicts the lowest current to be 2.5 kA with the *Cosine* pulse. According to the RMG model, high threshold spikes can be observed for $\frac{1}{2}$ *Cosine* at pulse durations between 100 μs and 400 μs.

Furthermore, we could show that the $\frac{1}{2}$ *Cosine* pulse triggered an action potential at the first depolarizing quarter wave, whereas for a *Cosine* pulse, it was triggered at the second depolarizing half wave of the

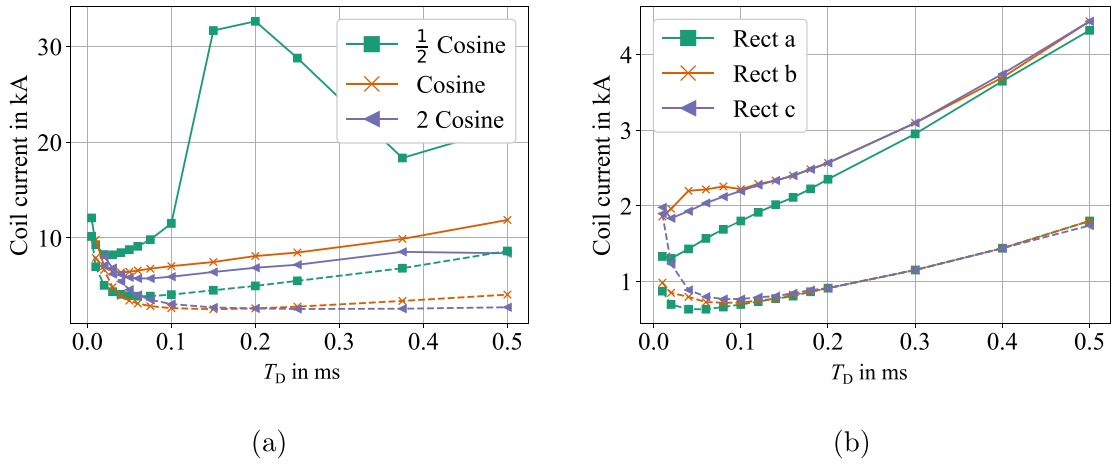

Figure 3. Strength duration curve for different stimulus shapes. The solid lines show data acquired using the RMG model and the dashed lines represent the MHH model. The *y*-axis for both plots shows the required coil current to trigger an action potential. Threshold coil currents are calculated based on equation (2). (a) shows the thresholds required for sinusoidal pulse shapes. (b) shows thresholds for rectangular pulse shapes. The depolarizing phase T_D of the pulse is defined as shown in figure 2.

Table 1. The lowest coil current triggering an action potential is evaluated at the pulse duration of the lowest threshold in the strength duration curve. Both, coil current and the corresponding pulse duration are listed below.

Stimulus	RMG		MHH	
	Current in kA	Pulse duration	Current in kA	Pulse duration
1/2 Cosine	8.2	30 μs	3.9	60 μs
Cosine	6.4	40 μs	2.5	150 μs
2 Cosine	5.7	75 μs	2.6	250 μs
Rect a	1.3	20 μs	0.6	50 μs
Rect b	1.8	10 μs	0.7	90 μs
Rect c	1.8	20 μs	0.8	90 μs

inverted field (see supplementary material). As soon as the field gets stronger, the depolarizing wave will elicit an action potential at the axon section with the positive peak in the activation function and the hyperpolarizing wave at the negative peak.

3.2. Rectangular pulses

In comparison to sinusoidal pulses, rectangular pulses require lower field strength to trigger an action potential at similar pulse durations. *Rect a*, *Rect b* and *Rect c* yield similar results. Optimal pulse duration and the corresponding coil current are listed in table 1. According to the RMG model the lowest threshold was 1.3 kA and can be achieved with *Rect a*. In contrast, the MHH model required a current of only 600A to perform a successful excitation.

We compared different pulse configurations and their influence on threshold for a 10 μs, 30 μs and 150 μs pulse, as shown in figure 4. A disadvantage concerning threshold occurs when both pulses are similar in time and intensity. The *Rect c* pulse of 150 μs with equal phases had a 16 times higher threshold than an ideal rectangular pulse of the same duration. Especially for short pulses, this relation is negligible.

3.3. Cross comparison

Further, we examined idealized temporal field shapes which are not associated to any stimulation devices. We considered sine-shaped pulses as well as ideal rectangular and triangular shapes. A visualization as well as the corresponding strength duration curves are provided in the supplementary material. We found that sine-shaped pulses have lower thresholds than cosine-shaped ones, whereas the former ones do not differ significantly among each other. An ideal rectangular pulse proved to be the most favourable one (RMG: 1 kA, MHH: 0.5 kA), especially as it does not show increasing thresholds for short pulse durations. The lowest threshold for each stimulus and the corresponding pulse durations and frequencies can be found in the supplementary material.

3.4. Pulse duration

Table 2 shows the values for the minimal achievable field strength and the pulse duration where twice of the minimal field strength is required. Those parameters are analogous to rheobase and chronaxie which are defined for ideal rectangular pulses. Values were estimated from the corresponding strength-duration curves (see supplementary material) of RMG and MHH model. Calculating the chronaxie time using equation (4) yields 198 μs.

Moreover, we found that ideal rectangular pulses as well as *Rect a* are solely charge dependent between 10 μs and 40 μs, since electric field intensity and pulse duration are indirectly proportional. For example, a pulse of 20 μs requires twice the field strength of a 40 μs pulse. Apart from that, we found that long pulse durations can block the propagation of an action

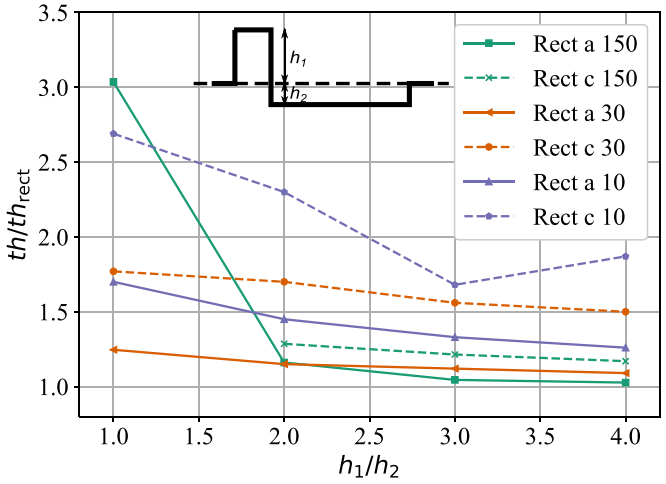

Figure 4. A realistic rectangular pulse consists of a positive and a negative pulse. Usually, one is short and high in intensity and the other one lower but longer. The duration of the first pulse was set to 150 μs and the height relation of the second was varied, which also changes the duration of the second pulse, described by the relation $\frac{h_1}{h_2}$. The influence of different height configurations is shown for *Rect a* and *Rect c* pulses of 10 μs, 30 μs and 150 μs. Thresholds are normed to an ideal rectangular pulse of the corresponding duration.

Table 2. Minimal achievable field strength and the duration at twice the minimal field strength are estimated from strength-duration curves (see supplementary).

Stimulus	Min. field in $\frac{V}{m}$		Duration at 2 × min. field in μs	
	RMG	MHH	RMG	MHH
1/2 Cosine	108	43	175	130
Cosine	119	41	160	159
2 Cosine	168	55	207	236
Rect a	86	36	108	100
Rect b	89	36	130	100
Rect c	89	35	130	113

Table 3. We varied the pulse duration for different axon diameters. The table shows the required coil current in kA for axon diameters of 12.8 μm, 8.7 μm and 5.7 μm in relation to an axon of 16 μm for pulse durations of 40 μs and 400 μs.

Pulse duration μs	12.8 μm	8.7 μm	5.7 μm
40 μs	1.32 kA	2.56 kA	7.40 kA
400 μs	1.32 kA	2.73 kA	8.00 kA

potential. Especially, rectangular pulses can cause a block (see supplementary material).

3.5. Axon diameter

Smaller axon diameters require increasing coil current. We showed a slight dependence on pulse width for different axon diameters, as shown in table 3. According to those results, thin axons are easier stimulated with short pulse durations.

Furthermore, we evaluated the impact of different stimulus types. We compared pulse shapes for axon diameters of 5.7 μm and 16 μm (see supplementary). For most stimulus shapes, differences were negligible. However, *Rect b* and *Rect c* showed 120% and 50% higher thresholds for a 5.7 μm axon, respectively.

4. Discussion

We created a simulation environment to evaluate effects of magnetic stimulation on peripheral nerves. The spatial field distribution was calculated for a *figure-of-8* and applied to two different neuronal models with varying axon diameters. Within this work, we investigated the temporal behaviour of the electrical field in order to optimize pulse duration and shape. Those parameters depend on the electric circuitry used in stimulation devices and might be chosen because of cost, feasibility or energy efficiency. We used two different neuronal models suitable for human peripheral nerves. The RMG double cable model provides great physiological accuracy at the cost of longer computation time [41]. Further, it was stated by [41] that it predicts higher thresholds which exceed experimental data. To put such potential offsets in relation, the MHH model was also introduced. Yet, for short pulse duration shorter than 40μs the RMG model provides more reliable data.

4.1. Stimulus comparison

Direct comparison of different stimulus shapes is hardly possible. Sinusoidal and rectangular pulses of the same duration apply different amounts of charge to the membrane capacity and the sequence of hyperpolarization and depolarization plays a crucial role [33].

A vast majority of stimulator devices available on the market use sinusoidal pulse shapes, either monophasic or biphasic, the latter allowing repetitive stimulation. We compared cosine-shaped electrical field

shapes induced by a half sine wave coil current, a sine wave and a double sine wave.

To compare different stimulus types we investigated the corresponding strength-duration curves using the duration of the depolarizing phase T_D. In electric stimulation, the strength-duration curves would decrease with increasing pulse duration. In case of magnetic stimulation, short pulse durations imply higher coil current frequency and hence, higher electric field strength. Thus, the coil current in the strength-duration curves was adjusted according to equation (2) yielding a golf club shape. Moreover, $\frac{1}{2}$ *Cosine*, *Cosine* and *2 Cosine* have different frequencies at the same pulse width, which is compensated as well using equation (2).

Comparing the three cosine-shaped stimuli at the same frequency the *Cosine* and *2 Cosine* would be twice as long and four time longer than the $\frac{1}{2}$ *Cosine*. However, despite this mismatch in pulse duration, the thresholds were not distinctly different. It has been stated that a hyper-polarizing quarter cycle followed by a depolarizing half cycle is an advantageous pulse configuration [33]. Lower thresholds for the *Cosine* stimulus compared to the $\frac{1}{2}$ *Cosine* were observed before [31, 33–35]. The reason was considered to be that biphasic stimuli might have lower thresholds due to the longer depolarizing time [33, 34]. We could show that an action potential is indeed triggered by the first depolarizing quarter cycle of a $\frac{1}{2}$ *Cosine* stimulus, whereas it is the second depolarizing half cycle for a *Cosine* stimulus. Hence, the active phase of a $\frac{1}{2}$ *Cosine* is the first depolarizing quarter cycle and for a *Cosine* it is the first depolarizing half cycle. Since the half cycle contains more energy it is more likely to trigger an action potential. Confirming this assumption the sine-shaped pulses, where the active phase is the first half-cycle, proved to have even lower thresholds (see supplementary). To achieve such a pulse, the coil current needs to be cosine-shaped, which has not yet been achieved to our knowledge.

However, comparing the three cosine-shaped stimuli at the same pulse duration the *2 Cosine* yields the lowest thresholds according to the RMG model. A reason for that is the high frequency of the pulse, which increases the field strength. In accordance to that, the *Cosine* had the second lowest thresholds.

High thresholds that cause spikes in the strength-duration curve with the RMG model are caused by blocked action potential propagation. For example, an action potential is triggered at one segment by the first depolarizing quarter wave of the $\frac{1}{2}$ *Cosine* and it starts propagating in both directions. Once the propagating action potential hits a segment which is at this time in the hyper-polarizing phase of the pulse, negative interference will cancel the action potential.

Rectangular stimulus shapes were already shown to be efficient for electrical stimulation [28]. We could show that rectangular pulse shapes have lower thresholds than cosine-shaped ones. However, a $\frac{1}{2}$ *Cosine* consists of a depolarizing and a hyper-polarizing quarter wave while the rectangular pulse has a strong depolarizing part and low hyper-polarization. Further, a rectangular pulse delivers more charge to the membrane capacity, since there is a small rising time due to the steep edge at the beginning and at the end of a pulse. In general, considering different rectangular configurations, we saw that strong hyper-polarization is not advantageous. Hence, a brief and high intensity pulse followed by a longer one with lower intensity seems to be the best configuration. A reason might be that hyper-polarization at the neighbouring Nodes of Ranvier blocks the propagation of the action potential. The absence of strong hyper-polarization might also be an advantage of the rectangular pulses compared to cosine-shaped ones. That argument is supported by the ideal rectangular pulse, which only has a depolarizing phase, and showed the lowest threshold of all pulses.

In general, rectangular pulses proved to require less current than cosine-shaped ones especially for short pulse durations, which is discussed later. Operating stimulation devices with only 600 A facilitates high switching rates which enables short pulses. Polyphasic cosine-shaped pulses like the *2 Cosine* come with rapid field switching for short pulses, although such configurations are hardly feasible due to circuitry limitations. Even at optimal pulse durations, currents of 2.5 kA are necessary. We further concluded, that a solely depolarizing pulse is the best option. Due to energy flow, such a configuration is not feasible, hence the hyper-polarizing phase should have as less intensity as possible.

4.2. Pulse duration

Usually, concerning magnetic stimulation, pulse duration mainly depends on stimulation coil and pulse capacitors. Recent stimulation devices allow to vary the pulse duration. As former studies have shown, the coil current can be reduced by choosing a proper pulse duration [16, 19, 22, 29, 32, 46]. We demonstrated how the required coil current changes with pulse duration. That is because shorter pulse durations require higher field strengths and further, because changing the pulse duration means a different current frequency, which again scales the electric field. The resulting curves of the analysis are generally golf club shaped, meaning the threshold increases slowly for long pulses and rapidly after the minimum for short pulse durations, especially for pulses with strong hyper-polarising part.

At short pulse durations, the hyper-polarizing phase of a pulse becomes more relevant. We could show that pulses with no or only few hyper-polarizing part, like the ideal rectangular and *Rect a* pulse, are solely charge dependent for pulse duration between 10 μs and 40 μs. As long as pulses are shorter than the

membrane time constant, which is defined by capacitance and resistance, the required field strength increases proportional to decreasing pulse duration. Within this time span, the membrane capacitance is charged and subsequently generates a membrane voltage change. Pulses longer than the time constant are less efficient, since energy is lost on the resistive part of the cell membrane. As a consequence, the threshold current for an ideal rectangular or *Rect a* pulse does not increase for short pulse durations. In contrary, cosine-shaped pulses will require increasing coil current for short pulse durations. That is because they consist of a depolarizing and an equally strong hyperpolarizing phase, which immediately discharges the membrane capacitance. If that happens within a time span shorter than the sodium channel activation time, no action potential is triggered. Hence, the hyperpolarizing phase is especially inconvenient for short pulse durations and should be as long and low in intensity as possible. This can be achieved using pulses such as the *Rect a*.

Chronaxie is considered to be a good measure for pulse efficiency, whereby pulses longer than chronaxie time are unfavourable [47]. We estimated the pulse duration where twice the minimal achievable current is required from the strength duration curve. This measure is inspired by the chronaxie time, which is defined as twice the rheobase current for rectangular pulses.

Rectangular pulses have twice the minimal current at durations around 100 μs, whereas $\frac{1}{2}$ *Cosine* and *Cosine* have 135 μs and the *2 Cosine*200 μs (RMG double cable model). The chronaxie time calculated based on the time constant τ is 285.7 μs which is in accordance with values from literature. Time constants of motor axons was determined to be 264(34)μs [32] or 343(127)μs [22]. Corresponding chronaxie times are 183μs and 238 μs, respectively.

However, the minimal required current according to our simulations proved to be at pulse durations distinctly shorter than chronaxie time. $\frac{1}{2}$ *Cosine* had an optimal T_D of 25 μs and *Cosine* as well as *2 Cosine* at 40 μs. Rectangular pulses only have increasing thresholds at pulse durations smaller than 90 μs and 20 μs according to the MHH model and the RMG model, respectively. As the RMG model is more precise, especially for short pulses, we can assume that rectangular pulses have an ideal pulse duration at 10 μs to 20 μs.

Available stimulation systems on the market using biphasic coil currents like PowerMag (Mag&More), MagPro (MagVenture), Brainsway or Neuronetics have pulse durations between 160 μs and 370 μs [15]. The depolarizing phase T_D is 80μs and 185 μs, respectively. According to our results, a T_D of 40 μs would be preferable. Short pulse durations using sinusoidal currents are challenging, as pulse frequency is limited by properties of coil and capacitor. Rapid current switching poses a general problem to devices operating with high voltages and currents. However, our results show that using rectangular pulses currents of as less as 1.3 kA are sufficient to stimulate peripheral nerves using rectangular pulses of 20 μs. As mentioned, the RMG model tends to predict thresholds higher than experimental data. Hence, data from the MHH might be more accurate, which would enable stimulation currents as low as 600 A. Such low currents would make it possible to develop devices which are capable of high current switching rates. Yet, our simulation experiments were conducted in saline solution which does not properly represent typical applications. Investigations involving a field distribution in tissue are still necessary to draw proper conclusions on threshold currents.

4.3. Axon diameter

Peripheral nerves usually contain a variety of different axons for many physiological functions. Decreasing axon diameter goes along with increasing threshold intensities [16, 41]. Ideally, thresholds for peripheral stimulation can be reduced as such that only the desired motor axons are stimulated. Therefore, it is crucial to know characteristic thresholds for distinct axon types. It has been reported that not only increasing stimulation distance but also shorter pulse duration increases the selectivity between axon diameters in electric stimulation [16]. In our experiments, we investigated different pulse durations for 5.7 μm and 16 μm axons. We could only see a slight decrease of threshold differences with decreasing pulse duration. However, the effect observed with electric stimulation might be due to impedance effects of the tissue which filters short pulse durations.

According to our findings, selective stimulation is hardly influenced by pulse shape or duration. Nevertheless, threshold differences between axon types are prominent and allow distinct stimulation of functional axon groups. An axon with a diameter of 5.7 μm requires six times higher thresholds than one with a thickness of 16 μm. In fact, a growing increase of threshold can be observed with decreasing diameter. Hence, smaller axons which are usually not target of magnetic stimulation are even less likely to be activated.

5. Conclusion

The goal of this study was to find the most energy efficient pulse-shape for magnetic neurostimulation. We have therefore evaluated several temporal pulse shapes with two biophysically plausible axon models. Asymmetric biphasic rectangular pulses, where the depolarizing phase duration was around 20 μs and the hyper-polarizing phase had at least a four-times smaller amplitude (and a four-times longer duration) required the smallest current to stimulate a target axon. The threshold current for this pulse to stimulate

an axon was as low as 600 A, which was four times smaller than for conventionally used cosine-shaped pulses. These findings motivate the development of new low current magnetic stimulating devices with rectangular pulses, which are less expensive, more compact devices and which reach a much higher energy efficiency. Novel therapeutical applications, where repetitive pulses are required, will become possible with lower coil currents due to reduced coil heating. Moreover, we conclude that low current stimulation devices are suitable for peripheral stimulation, since axons of large diameters, such as motor neurons, can be stimulated with lower field strengths. Unwanted stimulation of thin axons in the autonomous nervous system can be avoided.

Acknowledgments

Funding for this work was granted by the Deutsche Forschungsgemeinschaft (DFG, German Research Foundation), Project number DFG GL661/5-1.

ORCID iDs

J Rapp https://orcid.org/0000-0001-7187-6972
P Braun https://orcid.org/0000-0003-4486-7776
W Hemmert https://orcid.org/0000-0002-2905-6118
B Gleich https://orcid.org/0000-0002-0574-7678

References

[1] Wassermann E M, Grafman J, Berry C, Hollnagel C, Wild K, Clark K and Hallett M 1996 Use and safety of a new repetitive transcranial magnetic stimulator *Electroencephalography and Clinical Neurophysiology/Electromyography and Motor Control* **101** 412–7
[2] Gershon A A, Dannon P N and Grunhaus L 2003 Transcranial magnetic stimulation in the treatment of depression *The American Journal of Psychiatry* **160** 835–45
[3] Inaba A, Yokota T, Saito Y, Ichikawa T and Mizusawa H 2001 Proximal motor conduction evaluated by transcranial magnetic stimulation in acquired inflammatory demyelinating neuropathies *Clinical Neurophysiology* **112** 1936–45
[4] Rossini P M and Rossi S 2007 Transcranial magnetic stimulation: diagnostic, therapeutic, and research potential *Neurology* **68** 484–8
[5] Groppa S *et al* 2012 A practical guide to diagnostic transcranial magnetic stimulation: report of an ifcn committee *Clinical Neurophysiology : Official Journal of The International Federation of Clinical Neurophysiology* **123** 858–82
[6] Lefaucheur J P *et al* 2014 Evidence-based guidelines on the therapeutic use of repetitive transcranial magnetic stimulation (rtms) *Clinical Neurophysiology : Official Journal of the International Federation of Clinical Neurophysiology* **125** 2150–206
[7] Bersani F S *et al* 2013 Deep transcranial magnetic stimulation as a treatment for psychiatric disorders: a comprehensive review *European Psychiatry : The Journal of the Association of European Psychiatrists* **28** 30–9
[8] Kinoshita S, Ikeda K, Hama M, Suzuki S and Abo M 2020 Repetitive peripheral magnetic stimulation combined with intensive physical therapy for gait disturbance after hemorrhagic stroke: an open-label case series *International journal of rehabilitation research. Internationale Zeitschrift fur Rehabilitationsforschung. Revue internationale de recherches de readaptation* **43** 235–9
[9] Carrico C, Chelette K C, Westgate P M, Salmon-Powell E, Nichols L and Sawaki L 2016 Randomized trial of peripheral nerve stimulation to enhance modified constraint-induced therapy after stroke *American Journal of Physical Medicine & Rehabilitation* **95** 397–406
[10] Celnik P, Paik N J, Vandermeeren Y, Dimyan M and Cohen L G 2009 Effects of combined peripheral nerve stimulation and brain polarization on performance of a motor sequence task after chronic stroke *Stroke* **40** 1764–71
[11] HamnegÅard C H, Wragg S, Kyroussis D, Mills G, Bake B, Green M and Moxham J 1995 Mouth pressure in response to magnetic stimulation of the phrenic nerves *Thorax* **50** 620–4
[12] Similowski T, Mehiri S, Duguet A, Attali V, Straus C and Derenne J P 1997 Comparison of magnetic and electrical phrenic nerve stimulation in assessment of phrenic nerve conduction time *Journal of Applied Physiology (Bethesda, Md.: 1985)* **82** 1190–9
[13] Davids M, Guérin B, Klein V, Schmelz M, Schad L R and Wald L L 2020 Optimizing selective stimulation of peripheral nerves with arrays of coils or surface electrodes using a linear peripheral nerve stimulation metric *J. Neural Eng.* **17** 016029
[14] Olney R K, So Y T, Goodin D S and Aminoff M J 1990 A comparison of magnetic and electrical stimulation of peripheral nerves *Muscle & Nerve* **13** 957–63
[15] Yanamadala J, Borwankar R, Makarov S and Pascual-Leone A 2019 *Brain and Human Body Modeling: Computational Human Modeling at EMBC 2018: Estimates of Peak Electric Fields Induced by Transcranial Magnetic Stimulation in Pregnant Women as Patients or Operators Using an FEM Full-Body Model* (Cham: CH)
[16] Grill W M and Mortimer J T 1996 The effect of stimulus pulse duration on selectivity of neural stimulation *IEEE Transactions on Bio-Medical Engineering* **43** 161–6
[17] McIntyre C C, Richardson A G and Grill W M 2002 Modeling the excitability of mammalian nerve fibers: influence of afterpotentials on the recovery cycle *Journal of Neurophysiology* **87** 995–1006
[18] Pashut T, Wolfus S, Friedman A, Lavidor M, Bar-Gad I, Yeshurun Y and Korngreen A 2011 Mechanisms of magnetic stimulation of central nervous system neurons *PLoS Comput. Biol.* **7** e1002022
[19] Basser P J and Roth B J 1991 Stimulation of a myelinated nerve axon by electromagnetic induction *Medical & Biological Engineering & Computing* **29** 261–8
[20] Peterson E J, Izad O and Tyler D J 2011 Predicting myelinated axon activation using spatial characteristics of the extracellular field *J. Neural Eng.* **8** 046030
[21] Wang W T, Xu B and Butman J A 2017 Improved snr for combined tms-fmri: A support device for commercially available body array coil *J. Neurosci. Methods* **289** 1–7
[22] Mogyoros I, Kiernan M C and Burke D 1996 Strength-duration properties of human peripheral nerve *Brain : A Journal of Neurology* **119** 439–47
[23] Klinke R , Pape H-C, Kurtz A and Silbernagl S 2009 *Physiologie* ([Thieme]: Stuttgart)
[24] Gattinger N, Moessnang G and Gleich B 2012 Flextms–a novel repetitive transcranial magnetic stimulation device with freely programmable stimulus currents *IEEE Transactions on Bio-Medical Engineering* **59** 1962–70
[25] Peterchev A V, Jalinous R and Lisanby S H 2008 A transcranial magnetic stimulator inducing near-rectangular pulses with controllable pulse width (ctms) *IEEE Transactions on Bio-Medical Engineering* **55** 257–66
[26] Peterchev A V, Goetz S M, Westin G G, Luber B and Lisanby S H 2013 Pulse width dependence of motor threshold and input-output curve characterized with controllable pulse parameter transcranial magnetic stimulation *Clinical Neurophysiology : Official Journal of the International Federation of Clinical Neurophysiology* **124** 1364–72

[27] Goetz S M, Luber B, Lisanby S H, Murphy D L K, Kozyrkov I C, Grill W M and Peterchev A V 2016 Enhancement of neuromodulation with novel pulse shapes generated by controllable pulse parameter transcranial magnetic stimulation *Brain Stimul.* **9** 39–47
[28] Wongsarnpigoon A, Woock J P and Grill W M 2010 Efficiency analysis of waveform shape for electrical excitation of nerve fibers *IEEE transactions on neural systems and rehabilitation engineering : a publication of the IEEE Engineering in Medicine and Biology Society* **18** 319–28
[29] Panizza M, Nilsson J, Roth B J, Basser P J and Hallett M 1992 Relevance of stimulus duration for activation of motor and sensory fibers: implications for the study of h-reflexes and magnetic stimulation *Electroencephalography and Clinical Neurophysiology/Evoked Potentials Section* **85** 22–9
[30] Barker A T, Jalinous R and Freeston I L 1985 Non-invasive magnetic stimulation of human motor cortex *The Lancet* **325** 1106–7
[31] Kammer T, Beck S, Thielscher A, Laubis-Herrmann U and Topka H 2001 Motor thresholds in humans: a transcranial magnetic stimulation study comparing different pulse waveforms, current directions and stimulator types *Clinical Neurophysiology* **112** 250–8
[32] Maddison P, Newsom-Davis J and Mills K R 1999 Strength-duration properties of peripheral nerve in acquired neuromyotonia *Muscle & Nerve* **22** 823–30
[33] Maccabee P J, Nagarajan S S, Amassian V E, Durand D M, Szabo A Z, Ahad A B, Cracco R Q, Lai K S and Eberle L P 1998 Influence of pulse sequence, polarity and amplitude on magnetic stimulation of human and porcine peripheral nerve *The Journal of Physiology* **513** 571–85
[34] Niehaus L, Meyer B U and Weyh T 2000 Influence of pulse configuration and direction of coil current on excitatory effects of magnetic motor cortex and nerve stimulation *Clinical Neurophysiology* **111** 75–80
[35] Delvendahl I, Gattinger N, Berger T, Gleich B, Siebner H R and Mall V 2014 The role of pulse shape in motor cortex transcranial magnetic stimulation using full-sine stimuli *PLoS One* **9** e115247
[36] Havel W J, Nyenhuis J A, Bourland J D, Foster K S, Geddes L A, Graber G P, Waninger M S and Schaefer D J 1997 Comparison of rectangular and damped sinusoidal db/dt waveforms in magnetic stimulation *IEEE Trans. Magn.* **33** 4269–71
[37] Wang B, Grill W M and Peterchev A V 2018 Coupling magnetically induced electric fields to neurons: Longitudinal and transverse activation *Biophys. J.* **115** 95–107
[38] Lubba C H, Le Guen Y, Jarvis S, Jones N S, Cork S C, Eftekhar A and Schultz S R 2019 Pypns: multiscale simulation of a peripheral nerve in python *Neuroinformatics* **17** 63–81
[39] Rattay F 1989 Analysis of models for extracellular fiber stimulation *IEEE Transactions on Bio-Medical Engineering* **36** 676–82
[40] HODGKIN A L and HUXLEY A F 1952 A quantitative description of membrane current and its application to conduction and excitation in nerve *The Journal of Physiology* **117** 500–44
[41] Richardson A G, McIntyre C C and Grill W M 2000 Modelling the effects of electric fields on nerve fibres: influence of the myelin sheath *Medical & Biological Engineering & Computing* **38** 438–46
[42] Hines M L and Carnevale N T 1997 The neuron simulation environment *Neural Comput.* **9** 1179–209
[43] Aberra A S, Wang B, Grill W M and Peterchev A V 2020 Simulation of transcranial magnetic stimulation in head model with morphologically-realistic cortical neurons *Brain Stimul.* **13** 175–89
[44] Bossetti C A, Birdno M J and Grill W M 2008 Analysis of the quasi-static approximation for calculating potentials generated by neural stimulation *J. Neural Eng.* **5** 44–53
[45] Roth B J and Basser P J 1990 A model of the stimulation of a nerve fiber by electromagnetic induction *IEEE Transactions on Bio-Medical Engineering* **37** 588–97
[46] Hannah R, Rocchi L, Tremblay S and Rothwell J C 2016 Controllable pulse parameter tms and tms-eeg as novel approaches to improve neural targeting with rtms in human cerebral cortex *Frontiers in Neural Circuits* **10** 97
[47] Irnich W 1980 The chronaxie time and its practical importance *Pacing and Clinical Electrophysiology : PACE* **3** 292–301